DOI: 10.1002/ejic.200700978

A New Chemical Route to Synthesise TM-Doped (TM = Co, Fe) TiO_2 Nanoparticles

Manuel R. Nunes,[a] Olinda C. Monteiro,[a] Ana L. Castro,[a] Duarte A. Vasconcelos,[b] and António J. Silvestre*[b]

Keywords: Diluted magnetic semiconductors / Co- and Fe-doped TiO_2 anatase nanocrystallites / Hydrothermal synthesis / $TiCl_3$

Since the discovery of ferromagnetism well above room temperature in the Co-doped TiO_2 system, diluted magnetic semiconductors based on TiO_2 doped with transition metals have generated great interest because of their potential use in the development of spintronic devices. The purpose of this paper is to report on a new and swift chemical route to synthesise highly stable anatase single-phase Co- and Fe-doped TiO_2 nanoparticles, with dopant concentrations of up to 10 at.-% and grain sizes that range between 20 and 30 nm. Complementary structural, microstructural and chemical analyses of the different nanopowders synthesised strongly support the hypothesis that a homogeneous distribution of the dopant element in the substitutional sites of the anatase structure has been achieved. Moreover, UV/Vis diffuse reflectance spectra of powder samples show redshifts to lower energies and decreasing bandgap energies with increasing Co or Fe concentration, which is consistent with n-type doping of the TiO_2 anatase matrix. Films of Co-doped TiO_2 were successfully deposited onto Si (100) substrates by the dip-coating method, with suspensions of $Ti_{1-x}Co_xO_2$ nanoparticles in ethylene glycol.

Introduction

Titanium dioxide is a wide band-gap semiconductor that has potentially a large number of technological applications because of its excellent optical transmission in the visible and near-infrared regions, high refractive index, high dielectric constant and useful photocatalytic properties.[1] More recently, Co-doped TiO_2 has generated increasing interest as a diluted magnetic semiconductor (DMS) because of its ferromagnetic behaviour well above room temperature for low Co doping concentrations, and exhibits $T_c > 650$ K and one of the highest saturation magnetisations of any recently discovered DMS.[2–4] Moreover, ferromagnetism in TiO_2 resulting from oxygen vacancies and/or defects was also reported.[5,6] These properties make it a very promising material in the development of spintronic heterostructures by using highly spin-polarised semiconductors operating at room temperature.

The earliest observation of room temperature ferromagnetism in Co-doped TiO_2 was reported by Matsumoto et al.,[7] who synthesised anatase-phase $Ti_{1-x}Co_xO_2$ films ($0 \leq x \leq 0.08$) by combinatorial laser molecular beam epitaxy. A few months later, the same research group reported room-temperature ferromagnetism in rutile-phase $Ti_{1-x}Co_xO_2$ ($0 \leq x \leq 0.05$) films, by using the same deposition technique.[8] Since then, synthesis of anatase or rutile Co:TiO_2 films has been achieved by using several deposition techniques, e.g. oxygen plasma-assisted molecular beam epitaxy,[9] sputtering,[10] pulsed-laser deposition,[11,12] sol-gel techniques[13,14] and cathodic electrolytic deposition.[15] Besides Co, other transition metals (TMs) such as Fe, Cr or V were successfully used as dopant elements to induce room-temperature ferromagnetism in TiO_2 crystalline structures.[2,16]

Despite these achievements, there is a continuous search for synthesis methods that allow the growth of TM-doped TiO_2 thin films, which guarantee interface quality and compatibility with Si technology and other industrially relevant semiconductors. Endeavours are particularly focused on anatase single-phase synthesis since electron mobility is higher in anatase than in the rutile phase, and it is preferable for spin injection applications with Si.[17,18] However, anatase has a lower thermodynamic stability than the rutile structure. Furthermore, synthesis at high temperature should be avoided since the solubility of the dopant element is low at high temperature. Consequently, much attention is currently devoted to developing alternative synthesis processes.

Anatase TiO_2 nanoparticles have been obtained primarily by solution chemistry involving titanium sulfates and by

[a] Faculty of Sciences, University of Lisbon, Department of Chemistry and Biochemistry and CCMM,
Campo Grande, 1749-016 Lisboa, Portugal
Fax: +351-217500994
E-mail: mrnunes@fc.ul.pt
[b] Instituto Superior de Engenharia de Lisboa and ICEMS,
R. Conselheiro Emídio Navarro 1, 1959-007 Lisboa, Portugal
Fax: +351-218317138
E-mail: asilvestre@deq.isel.ipl.pt

hydrolytic reactions of titanium(IV) chloride or titanium organometallic compounds. These methods usually involve hazardous compounds and have shortcomings since chemical impurities or minor accessory phases are always present in the final products.[19] In this paper we report on a novel and swift chemical route to synthesise anatase single-phase Co- and Fe-doped TiO_2 nanocrystallites. Our synthesis approach is an extension of the hydrothermal process that uses a commercial solution of $TiCl_3$ as titanium precursor to prepare highly pure and stable anatase TiO_2 nanopowders, recently reported by A. L. Castro et al.[20] (see Experimental Section). Our method, relative to other methods, presents several advantages. The procedure is simple and low cost, it avoids the use of hazardous chemical compounds and it is a low-temperature synthesis technique. Furthermore, it allows the use of starting materials with high purity and to obtain a homogeneous mixture of two cations in the liquid state. Finally, it prevents the formation of undesirable secondary phases. Suspensions of Co-doped TiO_2 nanoparticles in water and in ethylene glycol were used to deposit $Ti_{1-x}Co_xO_2$ ($x \leq 0.1$) thin films onto Si (100) substrates by the dip-coating method.

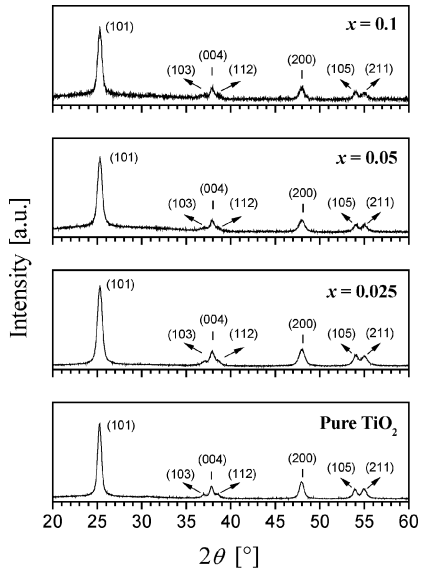

Figure 1. X-ray diffraction patterns of pure TiO_2 and $Ti_{1-x}Co_xO_2$ particle samples prepared with three different Co content.

Results and Discussion

Figure 1 shows a representative set of diffractograms recorded for pure TiO_2 and Co-doped TiO_2 nanopowder samples, with Co content that ranges from 2.5 to 10.0 at.-%. As can be seen, all the XRD patterns match the TiO_2 anatase phase JCPDS card no. 21–1272, which confirms that only one crystalline phase was formed during the synthesis process. No traces of rutile or brookite secondary phases were observed. Moreover, there is no sign of other undesirable phases throughout the whole range of cobalt content considered, e.g. cobalt clusters, cobalt oxides or Co–Ti oxide phases, which are known to exist in the bulk Co–Ti–O phase diagram.[21] This result seems to support the hypothesis that the dopant element is homogeneously distributed in substitutional sites of the anatase matrix as intended. The mean grain sizes of the samples were evaluated by Scherrer's equation,[22] with the (101) plane reflection at $2\theta = 25.281°$ and its full-width at half-maximum (FWHM), which was calculated by fitting the experimental diffraction lines with a Pseudo-Voigt function. Diffractograms of samples prepared with different dopant concentrations enabled us to estimate the mean grain sizes, which range between 20 and 30 nm.

To reinforce the assumption that the dopant element is homogeneously distributed in substitutional sites of the anatase structure, samples of pure TiO_2 and Co-doped TiO_2 nanoparticles with different Co content were also studied by TEM, electron diffraction and energy dispersive X-ray spectroscopy (EDS) and compared. For all Co concentrations tested ($x = 0.025$, 0.05 and 0.10), the $Ti_{1-x}Co_xO_2$ particles exhibit some heterogeneity in shape and size. Most are square or elongated nanocrystallites with a rather irregular surface microstructure that is similar to that observed for the pure TiO_2 anatase-phase samples, and without any microstructural evidence of the presence of other phases. Furthermore, the electron diffraction patterns of the $Ti_{1-x}Co_xO_2$ nanocrystallites are identical to those obtained for the pure anatase samples. These results are summarised in Figure 2, in which TEM micrographs of pure TiO_2 (Figure 2a) and $Ti_{0.95}Co_{0.05}O_2$ (Figure 2b) nanocrystal samples are shown. On the other hand, EDS spectra recorded over the $Ti_{1-x}Co_xO_2$ samples confirmed the presence of cobalt, with Co/Ti ratios close to the nominal stoichiometry values of the source solutions, as illustrated by the spectrum in Figure 3 obtained for a sample with $x = 0.05$. Furthermore, different EDS analyses scanning different regions of the powder samples showed no significant variations in the cobalt concentration, which attests to the homogeneous distribution of the dopant element all over the nanocrystals. Image analyses of the TEM micrographs showed average crystallite sizes consistent with the values determined by XRD.

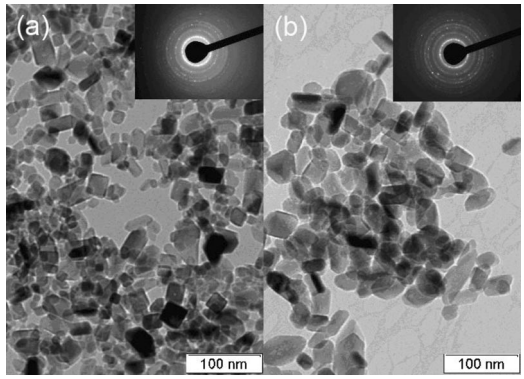

Figure 2. TEM micrographs of (a) pure TiO_2 and (b) $Ti_{0.95}Co_{0.05}O_2$ powder samples. The insets show electron diffraction patterns of the respective nanocrystalline samples.

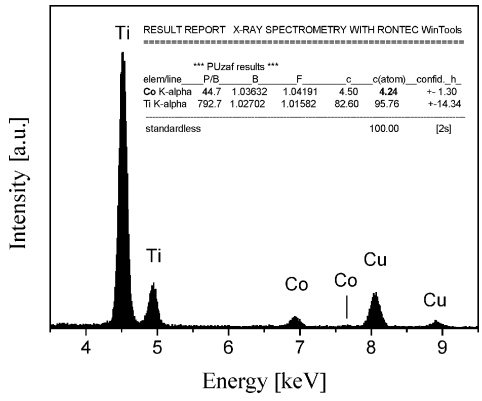

Figure 3. EDS spectrum of a $Ti_{0.95}Co_{0.05}O_2$ powder sample. The Cu peaks assigned are due to the copper grid used.

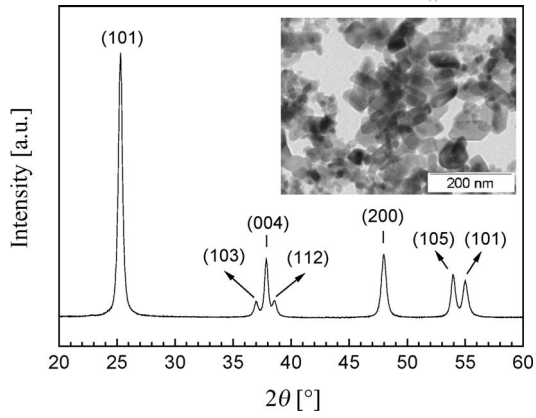

Figure 5. XRD pattern of a $Ti_{0.95}Fe_{0.05}O_2$ nanopowder sample. The inset shows a TEM micrograph of the same sample.

The effect of Co substitution on the TiO_2 anatase matrix was studied by examining the change in volume of the tetragonal unit cell ($V = a^2c$, where a and c are the lattice parameters) with doping concentration. Figure 4 shows the c-axis parameter and the cell volume as a function of Co content. As can be seen, as a consequence of the c parameter increase, the unit cell volume increases with x, in agreement with predictions for a Co-doped anatase matrix. Actually, cobalt appears in the doped TiO_2 system in the +2 formal oxidation state.[9] The ionic radii of Ti^{4+} and Co^{2+} are 0.68 Å and 0.82 Å, respectively. Consequently, substitution of Ti^{4+} by the larger Co^{2+} cation should expand the crystalline lattice and increase its volume.

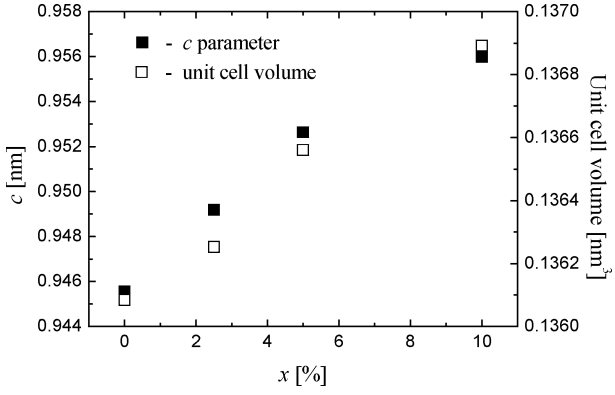

Figure 4. The c-axis parameter and the unit cell volume of $Ti_{1-x}Co_xO_2$ nanocrystallite samples as a function of the cobalt concentration.

The XRD patterns of the synthesised Fe-doped TiO_2 anatase nanopowders match that of the TiO_2 anatase phase without any trace of undesirable phases (Figure 5) and their microstructures are similar to those found for the Co-doped TiO_2 nanoparticles, with a slightly larger mean grain size (Figure 5, inset). No significant variation in the unit cell volume was observed for the Fe-doped TiO_2 samples, because Fe^{3+} has an ionic radius (0.64 Å) that is very close to that of Ti^{4+}.

Optical characterisation of undoped and doped TiO_2 powder samples was carried out by measuring the diffuse reflectance, R, at room temperature. R is related to the Kubelka–Munk function F_{KM} by the following relationship: $F_{KM}(R) = (1 - R)^2/2R$.[23] The bandgap energy of different $Ti_{1-x}TM_xO_2$ powders was calculated from their diffuse reflectance spectra by plotting the function $f_{KM} = (F_{KM}h\upsilon)^2$ versus energy (in electron volts). The linear part of the curves were extrapolated to $f_{KM} = 0$ to get the direct bandgap energy, E^d_g, of the samples. Figure 6 shows the plots for $Ti_{1-x}Co_xO_2$ samples with different Co concentrations. As can be seen, an increase in the doping concentration shifts the absorption edge to longer wavelengths (lower energies) and decreases the bandgap energy. A bandgap energy of 3.25 ± 0.01 eV was determined for a pure anatase TiO_2 sample, which is very close to 3.20 eV reported in literature for bulk anatase TiO_2. E^d_g values of 2.92 ± 0.01, 2.87 ± 0.02 and 2.80 ± 0.01 eV were estimated for $x = 0.025$, $x = 0.05$ and $x = 0.1$, respectively. Such redshifts of the absorption edge and the decrease in the bandgap energy with increasing Co content are consistent with the introduction of electronic states by the 3d electrons of the Co^{2+} cations, and therefore, with n-type doping of the TiO_2 anatase matrix.[24] A bandgap energy of 3.02 ± 0.01 eV was measured for the a sample with $x = 0.05$ for the Fe-doped TiO_2

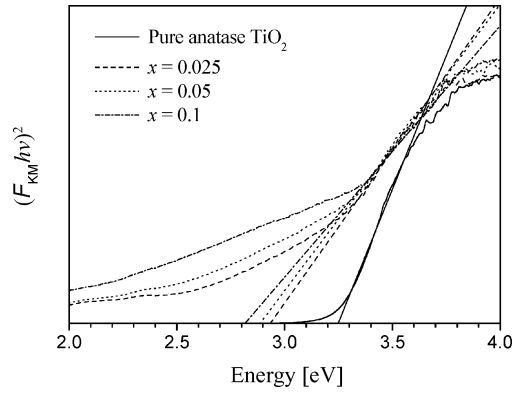

Figure 6. Diffuse reflectance spectra of different $Ti_{1-x}Co_xO_2$ powder samples.

powders (plot not shown); the observed redshift is attributed to the charge-transfer transition between the d electrons of the doping Fe^{3+} cation and the TiO_2 conduction band.[25]

With regard to the preparation of TM-doped TiO_2 films, we concentrated our efforts on the preparation of Co-doped TiO_2 thin films. Suspensions of $Ti_{1-x}Co_xO_2$ nanoparticles in water and in ethylene glycol (2 g dm^{-3}) were used to deposit Co-doped TiO_2 thin films onto Si (100) substrates by the manual dip-coating technique, followed by post-annealing at T = 200 °C in vacuo (ca. 10^{-2} mbar) for 30 min. SEM analyses showed that the microstructure of the films depend critically on the suspension medium used. Figure 7 shows two SEM micrographs of films prepared from suspensions of $Ti_{0.95}Co_{0.05}O_2$ nanoparticles in water and in ethylene glycol. As can be seen, the use of ethylene glycol as the suspension medium clearly prevents stress-related film damage: it stops films from cracking during either the drying or the final thermal curing stages and favours film homogeneity. Besides the dispersion medium, the pH of the suspension also seems to be an important experimental parameter that determines good film densification and homogeneity. Best results were obtained for acidified suspensions with nitric acid (pH ≈ 2), for which finer and more uniform particle dispersion was achieved. This result could probably be attributed to the double layer repulsion phenomena, which is well known to be responsible for the stability of colloidal systems.[26] The subject is currently being investigated.

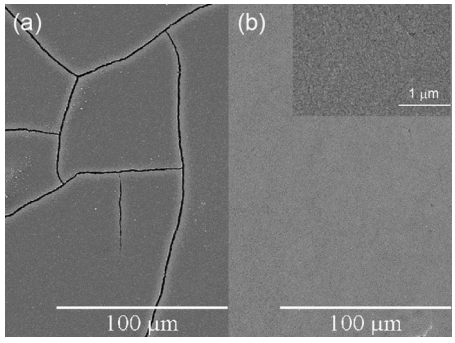

Figure 7. Deposition of Co-doped TiO_2 thin films onto Si (100) substrates prepared from acidified suspensions of $Ti_{0.95}Co_{0.05}O_2$ nanocrystallites in (a) water and (b) ethylene glycol. The inset shows a higher magnification detail of the microstructure of the film in (b).

Co-doped TiO_2 films prepared by using the experimental procedure described above are colourless and exhibit good adhesion properties. They have a dense granular microstructure, good surface coverage and retain the polycrystalline pure anatase structure of the precursor powders (Figure 8). It should be pointed out that Co-doped TiO_2 films grown on Si are always reported in the literature as exhibiting the rutile crystal structure, unless buffer layers are grown in between the substrate and the TiO_2 film.[2] Therefore, the procedure described here seems to be very promising when Co-doped TiO_2 anatase-phase films directly deposited onto silicon substrates are required.

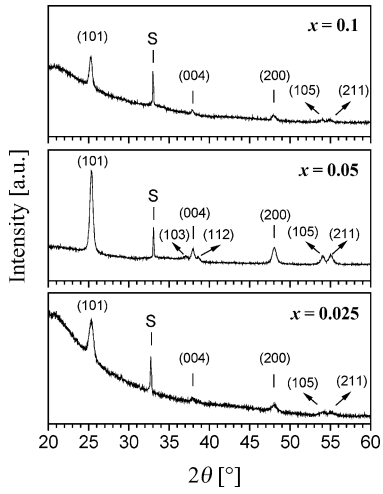

Figure 8. X-ray diffraction patterns of $Ti_{1-x}Co_xO_2$ thin films prepared with three different Co content. S refers to the peaks originating from silicon substrates.

Conclusions

A new and fast chemical route was developed to synthesise anatase single-phase TM-doped (TM = Co, Fe) TiO_2 nanoparticles. It was shown that pure and highly stable anatase $Ti_{1-x}Co_xO_2$ ($0 \leq x \leq 0.1$) nanopowders can be synthesised under low-temperature conditions, with mean grain sizes that range between 20 and 30 nm and with the dopant element homogeneously distributed in substitutional sites of the anatase matrix. Consistent with n-type doping, the UV/Vis diffuse reflectance spectra of representative powder samples have revealed redshifts to lower energies and decreasing bandgap energies with increasing TM concentration.

With the use of adequate suspension media, the nanopowders could have potential application in the deposition of $Ti_{1-x}Co_xO_2$ thin films at low temperatures, with either dip- or spin-coating techniques. In particular, films of Co-doped TiO_2 were successfully deposited onto Si (100) substrates by the dip-coating method, by using acidified suspensions of $Ti_{1-x}Co_xO_2$ nanoparticles in ethylene glycol.

Experimental Section

Nanoparticles Synthesis: All the reagents used in the synthesis experiments were purchased from commercial sources and used as received without further purification. A titanium trichloride solution (10 wt.-% in 20–30 wt.-% HCl, Aldrich) diluted in a ratio of 1:2 in standard (2 M) hydrochloride acid (37% HCl, Panreac) was used as the titanium source. To this solution, an ammonium solution (4 M) (Merck) was added dropwise under vigorous stirring, until complete precipitation of a white solid was observed. The resulting suspension was kept at rest for 15 h at room temperature and then filtered and vigorously rinsed with deionised water in order to remove the remaining ammonium and chloride ions. Crystallisation of the TiO_2 precursor was performed in an autoclave at 200 °C, for 6 h in an aqueous suspension. The same chemical route was used to synthesise TM-doped TiO_2, by adding the required molar amount of metallic cobalt or iron (Johnson Matthey) solu-

bilised in nitric acid to the titanium trichloride solution (doping step). After being washed, the undoped and doped TiO_2 nanoparticles can easily be stored in aqueous suspensions and straightforwardly retrieved by centrifugation whenever necessary. A flowchart of the overall synthesis method is shown in Figure 9.

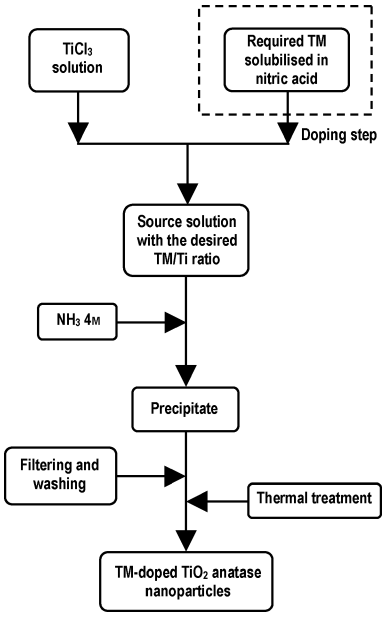

Figure 9. Flowchart of the synthesis method developed to prepare TM-doped (TM = Co, Fe) TiO_2 anatase nanoparticles. The same chemical route can be employed to prepare pure TiO_2 anatase phase, by using only the $TiCl_3$ solution.

Thin Film Preparation: $Ti_{1-x}Co_xO_2$ thin films deposited onto Si (100) substrates were prepared from suspensions of Co-doped TiO_2 nanoparticles in water and in ethylene glycol (2 g dm^{-3}), by the manual dip-coating technique, followed by post-annealing at 200 °C in vacuo (ca. 10^{-2} mbar) for 30 min. Before the dip-coating process, the substrates were cleaned with a 2% HF solution, then rinsed with deionised water and dried with blowing argon.

Characterisation: The crystallographic structure and phase purity of the powders were studied by X-ray diffraction (XRD) with Cu-K_α radiation, in the Bragg–Brentano (θ–2θ) geometry, by comparing the obtained patterns with the JCPDS database. The microstructure and morphology of the samples were analysed by TEM. The average crystallite size was evaluated from XRD data with the Scherrer equation and by TEM image analyses. In order to compare the nominal stoichiometry and the effective TM/Ti ratio, a set of representative doped samples were analysed by EDS. The optical characterisation of the powders was carried out by UV/Vis diffuse reflectance spectroscopy with a spectrophotometer equipped with an integrating sphere attachment. Spectra were recorded in the wavelength range 210–830 nm. The films prepared were analysed by XRD and SEM.

Acknowledgments

This work was financially supported by Fundação para a Ciência e Tecnologia (FCT) under the contract POCI/CTM/57019/2004. O. C. Monteiro acknowledges FCT for a post-doctoral grant (SFRH/BPD/14554/2003) and A. L. Castro acknowledges FCT for a PhD grant (SFRH/BD/19073/2004). The authors are very grateful to O. Conde and P. I. Teixeira for reading and commenting on this manuscript.

[1] U. Diebold, *Surf. Sci. Rep.* **2003**, *48*, 53–229.
[2] R. Janisch, P. Gopal, N. A. Spaldin, *J. Phys.: Condens. Matter* **2005**, *17*, R657–R689.
[3] S. R. Shinde, S. B. Ogale, S. Das Sarma, J. R. Simpson, H. D. Drew, S. E. Lofland, C. Lanci, J. P. Buban, N. D. Browning, V. N. Kulkarmi, J. Higgins, R. P. Sharma, R. L. Green, T. Venkatesan, *Phys. Rev. B* **2003**, *67*, 115211–115216.
[4] T. Fukumura, Y. Yamada, H. Toyosaky, T. Hasegawa, H. Koinuma, M. Kawasaki, *Appl. Surf. Sci.* **2004**, *223*, 62–67.
[5] N. H. Hong, J. Sakai, F. Gervais, *J. Magn. Magn. Mater.* **2007**, *316*, 214–217.
[6] S. D. Yoon, Y. Chen, A. Yang, T. L. Goodrich, X. Zuo, D. A. Arena, K. Ziemer, C. Vittoria, V. G. Harris, *J. Phys.: Condens. Matter* **2006**, *18*, L355–L361.
[7] Y. J. Matsumoto, M. Murakami, T. J. Shono, T. Hasegawa, T. Fukumura, M. Kawasaki, P. Ahmet, T. Chikyow, S. Y. Koshihara, H. Koinuma, *Science* **2001**, *291*, 854–856.
[8] Y. Matsumoto, R. Takahashi, M. Murakami, T. Koida, X.-J. Fan, T. Hasegawa, T. Fukumura, M. Kawasaki, S.-Y. Koshihara, H. Koinuma, *Jpn. J. Appl. Phys.* **2001**, *40*, L1204–L1206.
[9] S. A. Chambers, S. Thevuthansan, R. F. C. Farrow, R. F. Marks, J.-U. Thiele, L. Folks, M. G. Samant, A. J. Kellock, N. Ruzycki, D. L. Ederer, U. Diebold, *Appl. Phys. Lett.* **2001**, *79*, 3467–3469.
[10] W. K. Park, R. J. Ortega-Hertogs, J. S. Moodera, A. Punnoose, M. S. Seehra, *J. Appl. Phys.* **2002**, *91*, 8093–8095.
[11] Z. Wang, J. Tang, H. Zhang, V. Golub, L. Spinu, L. D. Tung, *J. Appl. Phys.* **2004**, *95*, 7381–7383.
[12] N. Popovici, E. Jiminez, R. C. da Silva, W. R. Branford, L. F. Cohen, O. Conde, *J. Non-Cryst. Solids* **2006**, *352*, 1486–1489.
[13] Y. L. Soo, G. Kioseoglu, S. Kim, Y. H. Kao, P. S. Devi, J. Parise, R. J. Gambino, P. I. Gouma, *Appl. Phys. Lett.* **2002**, *81*, 655–657.
[14] J. H. Cho, B. Y. Kim, H. D. Kim, S. I. Woo, S. H. Moon, J. P. Moon, J. P. Kim, C. R. Cho, Y. G. Joh, E. C. Kim, D. H. Kim, *Phys. Status Solidi* **2004**, *241*, 1537–1540.
[15] H. Wang, W. R. Branford, L. F. Cohen, S. J. Skinner, M. P. Ryan, *Chem. Mater.* **2007**, *19*, 3084–3086.
[16] J. M. D. Coey, *Curr. Opin. Solid State Mater. Sci.* **2006**, *10*, 83–92.
[17] T. Fukumura, H. Toyosaki, Y. Yamada, *Semicond. Sci. Technol.* **2005**, *20*, S103–S111.
[18] S. A. Chambers, T. C. Droubay, T. C. Kaspar in *Thin Films and Heterostructures for Oxide Electronics* (Ed.: S. B. Ogale), Springer, New York, **2005**, pp. 219–247.
[19] G. Li, L. Li, J. Boerio-Goates, B. F. Woodfield, *J. Am. Chem. Soc.* **2005**, *127*, 8659–8666, and references therein.
[20] A. L. Castro, M. R. Nunes, A. P. Carvalho, F. M. Costa, M. H. Florêncio, *Solid State Sci.*; DOI: 10.1016/j.solidstatesciences.2007.10.012.
[21] A. Yankin, O. Vikhreva, V. Balakirev, *J. Phys. Chem. Solids* **1999**, *60*, 139–143.
[22] B. D. Cullity and S. R. Stock, *Elements of X-ray Diffraction*, 3rd ed., Prentice-Hall, Inc., New Jersey, **2001**, pp. 170.
[23] G. Kortuem, *Reflectance Spectroscopy: Principles, Methods and Applications*, Springer-Verlag, New York, **1969**.
[24] M. Subramanian, S. Vijayalakshmi, S. Venkataraj, R. Jayavel, *Thin Solid Films* **2007**, DOI:10.1016/j.tsf.2007.06.125.
[25] M. S. Nahar, K. Hasegawa, S. Kagaya, *Chemosphere* **2006**, *65*, 1976–1982, and references therein.
[26] K. J. Mysels, M. N. Jones, *Discuss. Faraday Soc.* **1966**, *42*, 42–50.

Received: September 14, 2007
Published Online: December 3, 2007

